

1 Revision 1

## 2 **Magnetite spherules in pyroclastic iron ore at El Laco, Chile**

3  
4 JAN OLOV NYSTRÖM<sup>1,\*</sup>, FERNANDO HENRÍQUEZ<sup>2</sup>, JOSÉ A. NARANJO<sup>3</sup> AND H.  
5 RICHARD NASLUND<sup>4</sup>

6  
7 <sup>1</sup>Department of Geosciences, Swedish Museum of Natural History, SE-10405 Stockholm,  
8 Sweden

9 <sup>2</sup>Departamento de Ingeniería en Minas, Universidad de Santiago de Chile, 9170019 Santiago,  
10 Chile

11 <sup>3</sup>Servicio Nacional de Geología y Minería, Avda. Santa María 0104, 7550509 Santiago, Chile

12 <sup>4</sup>Department of Geological Sciences, SUNY, Binghamton, NY 13902-6000, U.S.A.

13  
14 \* E-mail: [jan.nystrom@nrm.se](mailto:jan.nystrom@nrm.se)

### 17 **ABSTRACT**

18  
19 The El Laco iron deposits in northern Chile consist of magnetite (or martite) and minor  
20 hematite, pyroxene and apatite. The orebodies are situated on a volcanic complex and resemble  
21 lavas and pyroclastic deposits, but a magmatic origin is rejected by some geologists who regard  
22 the ores as products of hydrothermal replacement of volcanic rocks. This study describes  
23 spherules of magnetite in the ore at Laco Sur, and outline a previously unrecognized  
24 crystallization process for the formation of spherical magnetite crystal aggregates during  
25 volcanic eruption.

26  
27 Mining at Laco Sur, the second largest deposit at El Laco, shows that most of the ore is  
28 friable and resembles pyroclastic material; hard ore with vesicle-like cavities occurs  
29 subordinately. The friable ore is a porous aggregate of 0.01-0.2 mm magnetite octahedra with  
30 only a local stratification defined by millimeter-thin strata of apatite. Films of iron phosphate are  
31 common on magnetite crystals, and vertical pipes called gas escape tubes are abundant in the ore.  
32 A SEM study reveals that magnetite spherules in the range 0.05-0.2 mm occur in most samples  
33 of friable ore from the central-lower part of the deposit. The proportion of spherules in a sample  
34 varies from high to nil, but overall the spherule content is low in the ore. The spherules are  
35 aggregates of octahedral crystals, or single octahedra, that have been rounded by stepwise,  
36 subparallel growth of magnetite with a systematic slight shift in orientation of successive steps.  
37 The shape of the spherules demonstrates that they formed unattached to any surface. Growth  
38 from hot magmatic gas saturated in iron in a volcanic plume and deposition as ash fall can  
39 account for the features of the spherule-bearing friable ore.

40  
41 **Keywords:** Crystal growth, Fe, eruption, magmatic gas, plume, volcanic ash

### 44 **INTRODUCTION**

46 The El Laco deposits are the best preserved examples of apatite iron ore of Kiruna type in  
47 the world. They occur on the flanks of a Plio-Pleistocene volcanic complex of andesitic to dacitic  
48 composition in the High Andes of northern Chile. There are seven deposits of high-grade iron  
49 ore within an area of 30 km<sup>2</sup>, with total resources exceeding 500 million tons (Fig. 1). The  
50 orebodies are composed of magnetite (or martite), and minor amounts of apatite, pyroxene and  
51 hematite.

52  
53 The first published report of the El Laco deposits (Park 1961) described the orebodies as  
54 magnetite lavas due to their morphological similarity to flows of vesicular basalt. Exploration  
55 trenching and mining subsequently revealed that much of the ore below the surface is friable and  
56 resembles pyroclastic material (Henríquez and Martín 1978; Nyström and Henríquez 1994;  
57 Naslund et al. 2002; Henríquez et al. 2003; Nyström et al. 2008). According to these authors the  
58 El Laco deposits formed from volatile-rich iron-oxide magmas that intruded the andesitic to  
59 dacitic volcanic structure at shallow depth and locally erupted to the surface.

60  
61 This magmatic interpretation has been questioned but the similarity in appearance of the ore  
62 to silicate lavas and pyroclastic material is not in dispute. Some authors believe that the El Laco  
63 deposits formed from iron-rich hydrothermal fluids that completely replaced silicate rocks whose  
64 volcanic structures and textures were inherited (Rhodes and Oreskes 1999; Rhodes et al. 1999;  
65 Sillitoe and Burrows 2002). Here we report new information that is inconsistent with a  
66 replacement origin.

67  
68 A SEM study of friable ore of pyroclastic appearance from one of the major orebodies, Laco  
69 Sur, reveals that ca. 0.1 mm diameter spherules of magnetite occur in most of the investigated  
70 samples. Such spherules have to the best of our knowledge not been reported before from iron  
71 deposits in the literature. The purpose of this paper is to describe these spherules, and to show  
72 that they formed by rapid crystal growth in a volcanic plume during eruption of iron-oxide melt.

73  
74

## 75 THE FRIABLE ORE

76

77 Laco Sur is the second largest deposit at El Laco (Fig. 1) and the only deposit that has been  
78 exploited. Mining has taken place intermittently, leaving a c. 150 m long open pit (Fig. 2). The  
79 pit wall is c. 25 m high in the central part of the section, where it consists of four benches, and  
80 lower at the sides. The appearance and physical character of the exposed ore varies considerably.  
81 Portions of the ore are hard and contain 1-15 mm large, often elongated open spaces similar to  
82 vesicles. This ore type is resistant to erosion and corresponds to the “magnetite lava” reported by  
83 Park (1961). However, the major part of the exposed ore in the open pit is friable. The spherules  
84 described in the present study occur only in the friable ore type.

85

86 The friable ore is a porous aggregate of fine-grained magnetite octahedra. The crystals are  
87 mainly between 0.01 and 0.1 mm in diameter, although some are 0.2 mm wide. The magnetite is  
88 unaltered in the open pit except near the upper surface and along steep faults where the oxidation  
89 to hematite is considerable to strong; martitized ore is not included in this study. Apatite  
90 (fluorapatite, Naslund et al. 2002) is another constituent of the ore, present in small to trace  
91 amounts. It occurs in two ways: as microscopic euhedral prisms which commonly are unbroken

92 and adhere to magnetite crystals, and as needles projecting from magnetite crystals in porous ore  
93 and vesicle-like cavities. Some cavities are white due to an abundance of apatite needles.

94  
95 Most of the friable ore lacks discernible structure or shows only a local, faint stratification  
96 (Fig. 3A). However, in some places a conspicuous stratification defined by millimeter-thin strata  
97 rich in apatite prisms can be followed for a few meters (Figs. 3B-C); cross-bedding is also  
98 observed (Fig. 3D). Stratified ore of different character is found in a roadcut 100-200 m  
99 southwest of the open pit (Fig. 1). The ore beds here are more extensive. They are size-sorted,  
100 lack visible apatite, and consist of euhedral to anhedral hematite crystals and crystal aggregates  
101 of coarser grain size than the friable magnetite ore in the open pit.

102  
103 From a distance, planar structures that extend for several meters to tens of meters and  
104 resemble bedding planes, can be distinguished in the pit wall (Fig. 2). They are subhorizontal or  
105 dip up to 30° away from the massive ore outcropping above the open pit (Fig. 1). The planar  
106 structures in the lowest bench are partly outlined by white inclusions of altered volcanic rock.  
107 Such inclusions are more common, and larger, outside the central section of the open pit. The  
108 rock inclusions show knife-sharp contacts towards the ore (Naslund et al. 2002). Inclusions of  
109 massive ore are also found, but their quantity is difficult to estimate due to often small textural  
110 contrasts with surrounding friable ore.

111  
112 The friable ore has a black to dark gray color. However, a dark green tone caused by a thin  
113 film of iron phosphate (lipscombite,  $\text{Fe}^{2+}\text{Fe}^{3+}_2(\text{PO}_4)_2(\text{OH})_2$ ) on the magnetite crystals is common  
114 in the central part of the open pit. Locally, the color of the film varies from iridescent blue to  
115 purple due to the presence of other, undetermined iron phosphates. A few, up to 1 cm large,  
116 flattened lumps of orange diadochite,  $\text{Fe}^{3+}_2(\text{PO}_4)(\text{SO}_4)(\text{OH})\cdot 6\text{H}_2\text{O}$ , are observed in the ore (Fig.  
117 3C). Diadochite is widespread in the stratified ore in the road cut southwest of the open pit  
118 (Naslund et al. 2002).

119  
120 The consolidation of the friable ore in the open pit is extremely variable. In places, the ore is  
121 an almost unconsolidated aggregate that easily crumbles into its constituents. In other places it  
122 grades into hard, dense ore. One controlling factor for this change is the proximity to open  
123 vertical pipes referred to as gas escape tubes (Figs. 3C and 4A-B). Such pipes are a characteristic  
124 feature of the friable ore in the open pit. They are meters to tens of meters long, and centimeters  
125 to tens of centimeters in diameter, with circular to oval cross sections (Naslund et al. 2002).  
126 Some of these open channels are more fissure-like than tubular and cross the entire 25 m high  
127 section.

128  
129 The interior surfaces of the gas escape tubes are partly coated by large magnetite octahedra  
130 with curved surfaces (Fig. 4B). Strongly altered prisms of pyroxene, and empty molds after this  
131 mineral revealed by occasional relicts, also line some tubes. In addition, pyroxene is intergrown  
132 with magnetite and minor apatite in a few veins cross-cutting the ore body. With the exception of  
133 these occurrences, pyroxene appears to be absent in the friable ore exposed in the open pit.  
134 However, drill cores from Laco Sur and other deposits in the district show that up to 3 cm long  
135 prisms of pyroxene occur as radiating prisms in rims around inclusions of altered rock, and as a  
136 matrix mineral at depth in the ore (Naranjo et al. 2010).

## MAGNETITE SPHERULES

Small spherical to spheroidal particles of magnetite, here referred to as spherules, were found during an inspection of friable ore from Laco Sur under a stereomicroscope. A systematic study was then made of all ore samples from the open pit at Laco Sur collected by one of us (JON), using a Hitachi S-4300 scanning electron microscope (accelerating voltage = 6 kV, beam current = 10  $\mu$ A) at the Swedish Museum of Natural History in Stockholm. It resulted in the discovery of spherules in 13 out of 17 investigated samples of friable ore of different texture and apatite content. Occurrence of spherules appears to be unrelated to the presence or absence of stratification or apatite content; apatite is abundant, sparse or absent in these samples. No spherules were found in the ‘vesicular’ ore type corresponding to the “magnetite lava” of Park (1961). All investigated samples of friable ore show a limited range in grain size, and lack inclusions of coarser material.

The magnetite spherules have diameters between 0.05 and 0.2 mm, the majority being 0.1-0.15 mm in diameter. Their form varies from almost spherical to ellipsoidal bodies, often with concavities (Figs. 5A-B). Some spherules with two concavities look like short cylinders or drums (Fig. 5C). The spherules occur mixed with aggregates and single crystals of octahedral magnetite of the same size range as the spherules (Figs. 5D-F). The main visible difference between octahedral aggregates and spherules is the rounded form of the latter. Particle aggregates approximately 0.1 mm in diameter consisting of up to ten small spherules joined together have been observed but are uncommon. The proportion of spherules varies: no sample consists solely of spherules; a few samples are dominated by spherules, but most contain a low proportion of spherules, and some lack spherules entirely. Overall, the content of spherules is low in the 17 investigated samples.

The spherules are aggregates of octahedral crystals (Figs. 6A-B), or single octahedra, that have been rounded by stepwise, subparallel growth of magnetite. A systematic slight shift in orientation of the individual steps constituting the overgrowth has generated curved crystal faces. They mimic the curved faces of large magnetite octahedra coating gas escape tubes (Fig. 4B). The outer surface of a spherule with subparallel overgrowth may be rather smooth (Fig. 5A), or have a morphology that is jagged in detail (Figs. 6C-D). Concavities are parts of spherules with less or no overgrowth. They reveal that the crystals in the aggregate below the overgrowth as a rule are coarser than the partial rim of overgrown crystals (Figs. 6B-C). With the exception of this rim, the spherules lack internal layering.

In three of the samples the crystal faces of magnetite octahedra are decorated with tiny projecting magnetite lamellae of bladelike form. The up to 0.1  $\mu$ m thick lamellae occur single (Fig. 6E) or grouped closely together in bands along octahedral planes (Figs. 6F and 7A). These projecting bands give a rough texture to the crystal surfaces. In addition, bladelike magnetite lamellae of different orientation form small rosettes on the octahedra (Fig. 6E), and on apatite prisms (Fig. 7B). However, most of the bladelike magnetite lamellae on apatite are predominantly oriented along its *c*-axis. Moreover, 10-25  $\mu$ m clusters of 0.1-0.5  $\mu$ m thick euhedral plates of hematite occur as local overgrowths on decorated magnetite octahedra (Fig. 6F).

184  
185  
186  
187  
188  
189  
190  
191  
192  
193  
194  
195  
196  
197  
198  
199  
200  
201  
202  
203  
204  
205  
206  
207  
208  
209  
210  
211  
212  
213  
214  
215  
216  
217  
218  
219  
220  
221  
222  
223  
224  
225  
226  
227  
228  
229

None of the other investigated samples have projecting lamellae of magnetite and clusters of hematite plates on octahedral faces. The magnetite in these samples may have a thin coating of precipitated silica, sparsely sprinkled with tiny droplike bodies of the same composition (Figs. 6C-D), or a patchy crust composed mainly of silica. Samples cemented by silica are relatively hard and come from the vicinity of gas escape tubes. Some magnetite crystals in samples at gas escape tubes have a corroded appearance.

One spherule looks different from all the others observed in this study. It is an aggregate of magnetite platelets (Fig. 7C). High magnification reveals the same projecting bladelike lamellae of magnetite and clusters of hematite described above. The morphology of the platelets appears to be the result of parallel twinning (cf. Fregola et al. 2005). These platelets differ in appearance from the platy magnetite made up of octahedra in parallel intergrowth reported by Nyström and Henríquez (1994, fig. 7D). Such thin plates were also found in this study, especially in samples without spherules. They look like single octahedra preferentially grown in one direction (Fig. 5B).

The composition of the magnetite was not determined in this study, leaving the question of chemical differences between magnetite in spherules and octahedral aggregates unexplored. A previous study (Nyström and Henríquez 1994) shows that magnetite at El Laco is rather uniform in composition.

## DISCUSSION

### Spherules of different origins

Magnetic spherules of similar dimension as those discovered at El Laco have been recovered from many environments, for example deep-sea sediment, polar ice, and areas with heavy industry. These spherical to subspherical particles are magnetite-bearing and can be of extraterrestrial, anthropogenic and, less commonly, volcanic origin.

Cosmic spherules (Genge et al. 2008) form by melting of micrometeorites. There are two types rich in iron: spherules composed predominantly of magnetite and wüstite, and spherules consisting of magnetite dendrites in silicate glass. Ablation of meteorites and impact events can also produce iron-rich spherules. The magnetite typically occurs as dendrites or dendritic arrays in these spherules (Zbik and Gostin 1995; Marini et al. 2004; Stankowski et al. 2006; Genge et al. 2008), in contrast to the octahedral aggregates at El Laco.

Anthropogenic spherules, formed by melting, are now found everywhere as contamination. They are present in fly ash, a waste material generated from the combustion of coal, and in emissions from metallurgical, metal-processing and other industries. Fly ash is characterized by a prevalence of spherical particles consisting of glass matrices with spinel minerals and silicates. The spinel phase is mostly magnetite, occurring as feathery or fanlike dendrites and octahedra (Sokol et al. 2002; Sulovsky 2002).

230 Spherules can also form from low-viscosity magmas erupting in fire fountains (Lefèvre et al.  
231 1986; Meeker and Hinkley 1993). These spherules consist largely of glass and their magnetite  
232 content is low. No silicate glass has been observed in the spherules from the open pit at Laco  
233 Sur, and basalts or other rocks from low-viscosity magmas are unreported from the volcanic  
234 complex hosting the ores. Iyer et al. (1999) suggested that magnetite-rich spherules found in  
235 pelagic clay from the Indian Ocean are volcanogenic-hydrothermal in origin. However, their  
236 argument against a cosmic origin rests solely on geochemical grounds.

237  
238

### 239 **A model for the formation of spherules at El Laco**

240

241 The magnetite spherules discovered at El Laco formed in a volcanic environment. The shape  
242 of the spherules demonstrates that they grew unattached to any surface, and their crystalline  
243 nature rules out formation of their spherical shape by abrasion. They crystallized in a medium  
244 that permitted unimpeded growth in all directions, which means a melt or fluid. It is very  
245 unlikely that the spherules crystallized in an iron-rich melt below the surface because their  
246 delicate features would not have survived an eruption undamaged, nor would the discrete apatite  
247 prisms coexisting with spherules in friable ore. Neither the apatite prisms nor the spherules have  
248 a surface coating as might be expected if they had been ejected from a melt and had retained a  
249 thin layer of melt on their surface (a silica coating, when present, is a late feature). Spherules  
250 have not been observed in orebodies morphologically similar to lava flows at El Laco. Thus,  
251 formation in a fluid or gas phase is indicated.

252

253 The hydrothermal models for the origin of the El Laco ore put forward by Rhodes and  
254 Oreskes (1999), Rhodes et al. (1999), and Sillitoe and Burrows (2002) are unable to explain the  
255 formation of unconsolidated ore containing spherules. The lack of attachment surfaces, the  
256 growth morphology, and the internal crystal texture of the spherules preclude formation by  
257 replacement or post-depositional recrystallization. Rhodes and Oreskes (1999) and Rhodes et al.  
258 (1999) proposed a multistep model in which andesite is replaced by scapolite, followed by  
259 pyroxene, which is in turn replaced by magnetite, without destruction of the original volcanic  
260 structures and textures. However, a study of drill cores from ore at depth in the area north of  
261 Laco Sur (Pasos Blancos; Fig. 1) by Naranjo et al. (2010) shows that the reverse took place:  
262 pyroxene formed after the main body of magnetite, and scapolite formed after (or together with)  
263 pyroxene.

264

265 We suggest that growth from hot, iron-saturated, magmatic gas in a volcanic eruption  
266 column accounts for the features of the spherule-bearing friable ore. The postulated existence of  
267 iron-oxide magma at a geologically realistic temperature requires large amounts of dissolved  
268 volatiles (Gibbon and Tuttle 1967; Weidner 1982), which are released during an eruption.  
269 Nyström et al. (2008) inferred a melt temperature of the order of 1000°C based on oxygen  
270 isotope data for magnetite from El Laco. Pyroxene, a late stage mineral in some of the ore,  
271 records temperatures in excess of 800°C in some samples, based on fluid inclusion  
272 homogenization (Broman et al. 1999; Rhodes et al. 1999) and pyroxene Ca-Fe-Mg exchange  
273 geothermometry (Lindsley 1983; Naslund et al. 2002). Large volumes of released volatiles are  
274 consistent with the widespread occurrence of apatite and iron phosphates in the porous, friable  
275 ore of the open pit. The apatite prisms in stratified ore probably formed from elemental

276 phosphorus in the eruption column. The dark green film of lipscombite on magnetite is pervasive  
277 in large portions of the friable ore. The abundance of gas escape tubes in this ore type bear  
278 witness of vigorous degassing of the iron-oxide magma.

279  
280 Crystallization of magnetite is believed to have started immediately on eruption in the  
281 expanding and cooling column. Experiments have established that magnetite crystallizes rapidly  
282 on quenching in Fe-rich melts and that no iron-oxide glass forms even at cooling rates >  
283 100°C/sec (Philpotts 1967; Naslund 1983), in contrast to volcanism involving silicate magmas,  
284 where glass is produced by quenching under analogous conditions.

285  
286 The friable ore in the open pit has a grain size corresponding to fine ash. The limited size  
287 range of the magnetite crystals, crystal aggregates and spherules in the samples, and the local  
288 stratification, suggest gravitational sorting. Variations in eruption intensity could account for the  
289 millimeter-thin strata defined by apatite. Rapid crystallization of magnetite from innumerable  
290 nuclei in the eruption column might also explain the limited size range of the magnetite.

291  
292 The magnetite crystals and crystal aggregates composing the friable ore could to a large  
293 extent be quenched, small droplets of iron-oxide melt. However, the spherules, or at least the  
294 overgrowth of subparallel magnetite that enhances their rounded form (Figs. 5A and 6C), and the  
295 finest ash particles probably crystallized from the magmatic gas driving the eruption.

296  
297 Experimental data support the idea that hot magmatic gas could carry considerable amounts  
298 of iron as halogen complexes. Experimental studies indicate that dilute chloride solutions at  
299 500°C can contain in excess of 1000 ppm Fe (Helz 1971), 1M HCl at 600°C may contain in  
300 excess of 40,000 ppm Fe (Whitney et al. 1985), and that concentrated chloride solutions at  
301 500°C can contain in excess of 100,000 ppm Fe (Chou and Eugster 1977). The predominance of  
302 fluorine over chlorine in halogen-bearing minerals at El Laco (Naranjo et al. 2010) strongly  
303 suggests that fluorine complexes played the principal role. Given the corrosive nature of HF  
304 solutions, there are little data on Fe solubilities in F-rich solutions at high temperature. At  
305 ~100°C, however, Fe concentrations in excess of 90,000 ppm can be obtained by dissolving  
306 FeSiF<sub>6</sub>·6H<sub>2</sub>O in water (Perry 2011). Any fluid or gas exsolved from an iron-oxide magma before  
307 or during an eruption would necessarily be saturated in iron. The changes in pressure and  
308 temperature associated with an eruption, however, are likely to cause dissolved iron to sublime  
309 directly from a fluid/gas phase into solid magnetite. Precipitation of magnetite and hematite by  
310 sublimation from hot volcanic gas is a common feature in the upper parts of siliceous ignimbrites  
311 (McBirney and Williams 1979).

312  
313 Large volumes of porous white rock of low density that consist almost exclusively of  
314 siliceous material outcrop between Laco Sur and Laco Norte (Fig. 1). It is an intensely leached  
315 volcanic rock. Leaching on such scale is consistent with an environment permeated by  
316 hydrofluoric acid. The molds after pyroxene at gas escape tubes also reflect the action of  
317 hydrofluoric acid.

318  
319 The hot magmatic gas driving the eruption was probably ejected at high speed (cf. Sparks et  
320 al. 1997). Gas flow within the column and during the eruption could have varied from laminar to  
321 turbulent. Flow variations and collisions of particles within a turbulent eruption column might

322 result in different spherule morphologies: rounded in some samples (Figs. 5A-B), angular in  
323 others (Fig. 5F), and even cylindrical (Fig. 5C).

324

325 The spherules at El Laco contain no silicate glass, and the octahedra composing them (Figs.  
326 6A-C) lack the ordered arrangement visible on the surface of spherules of cosmic origin  
327 consisting largely of magnetite (cf. fig. 3d in Stankowski et al. 2006, and fig. 2:1 in Marini et al.  
328 2004). The two quoted figures show skeletal crystals formed by continued crystallization of  
329 dendrites. The spherules at El Laco are aggregates of octahedra, not skeletal crystals. The  
330 spherules of cosmic origin formed from ‘super-heated’ glass, which would, as such, be devoid of  
331 any crystal nuclei and would be likely to result in dendritic growth. The El Laco melt was never  
332 super-heated, and as a result, likely retained sufficient crystal nuclei to form octahedral crystals  
333 upon cooling, even when quenched.

334

335 The formation of magnetite rather than hematite indicates a low oxygen fugacity during  
336 crystallization. Water was either absent or present in very low concentration in the eruption  
337 column, or the volcanic gas was buffered at an oxygen fugacity within the stability field of  
338 magnetite. The presence of S-SO<sub>2</sub>, CO-CO<sub>2</sub>, or H-HF in the gas stream could have acted as such  
339 a buffer. The dry environment and small size of magnetite crystals in the eruption column might  
340 mean that electrostatic forces influenced the growth of crystal aggregates (cf. Sparks et al. 1997).  
341 The stratified, size-sorted ore in the roadcut southwest of the open pit that consists of hematite  
342 (Fig. 7D) was deposited during a different style of eruption or from another vent than the ore in  
343 the open pit.

344

345 It is likely that magnetite crystals and apatite prisms formed in the eruption column settled  
346 out as fine ash and gave rise to the thick pyroclastic deposit of friable ore now exposed in the  
347 open pit. A few of the investigated samples were collected in parts of the ore pile penetrated by  
348 hot magmatic gas which resulted in dendritic overgrowths of magnetite: the magnetite lamellae  
349 decorating crystal surfaces (Figs. 6E to 7B). These dendrites apparently grew after the deposition  
350 of the ore, as shown by the fact that *all* crystals are decorated with dendrites in the only samples  
351 where they occur; *none* of the magnetite crystals in other samples are decorated with dendrites.

352

353 With increasing oxygen fugacity and/or lower temperature hematite became the stable phase  
354 and crystallized as clusters of small plates (Fig. 6F). The magnetite dendrites and hematite  
355 clusters enhanced the rounded form of the spherules. The apatite needles projecting from  
356 magnetite crystals in friable ore and occurring in cavities, and the apatite crystals in gas escape  
357 tubes and in late veins appear to have crystallized from a residual gas/fluid phase.

358

359 The deposited magnetite ash was sufficiently unconsolidated to be blown out locally by  
360 streaming gas. Subsequently, a few of the gas escape tubes were partially filled with bedded fine-  
361 grained magnetite. The fact that the 25 m high central section of the open pit contains many gas  
362 escape tubes, some crossing the entire section, strongly suggests that most of the ore in the open  
363 pit is pyroclastic. Magnetite from the vicinity of gas escape tubes is somewhat corroded.  
364 Deposition of silica at a late stage cemented the ore near open channelways.

365

366 The “magnetite flow” reported by Park (1961) is situated above the open pit (Fig. 1). The  
367 lava-like ore is very hard and might have protected the friable ore from erosion. Part of the



368 “flow” looks like a dike with vertical gas escape tubes along a planar surface (fig. 7 in Park  
369 1961). Henríquez and Martin (1978) interpreted this ore dike as a feeder for the flow. Other  
370 evidence for eruption of gas-rich iron-oxide melt at El Laco are spindle-shaped magnetite bombs  
371 (Henríquez and Nyström 1998) and scoriaceous ore (Naslund et al. 2002).

372  
373 It is possible that the eruption forming the ore exposed in the open pit at El Laco took place  
374 in a glaciated environment (Ammann et al. 2001; Naranjo et al. 2010). However, even eruptions  
375 that start under thick extensive ice sheets can evolve into sub-aerial eruptions with much ash.  
376 Such an eruption would border on magmato-phreatic and would have a variety of features not  
377 seen in the open pit. For example, a subglacial eruption is likely to have hematite in place of  
378 magnetite, as a result of alteration during cooling in a wet environment, and would be likely to  
379 have a clay-sized matrix.

380  
381 Most of the samples of friable ore contain spherules, and this ore type makes up the  
382 predominant part of the exposed ore in the open pit. A genetic model for El Laco must be able to  
383 explain the formation of the spherule-bearing, friable ore simultaneously with the formation of  
384 the deposit. Pyroclastic deposits composed of magnetite or hematite ash is not an ore type unique  
385 to El Laco. A recently described example is the Oligocene La Perla deposit in Mexico which  
386 even contains well-preserved fossil pollen in the pyroclastic ore (Corona-Esquivel et al. 2010),  
387 confirming surface deposition as unconsolidated ash at near ambient temperatures.

388  
389

## 390 **IMPLICATIONS**

391  
392 A previously unrecognized crystallization process for the formation of spherical  
393 magnetite crystal aggregates has been described. The magnetite spherules discovered in friable  
394 iron ore at Laco Sur formed by rapid crystal growth in hot, iron-saturated magmatic gas exsolved  
395 from an iron-oxide melt. The occurrence of spherules in unconsolidated, locally stratified and  
396 even cross-bedded deposits of 0.01-0.2 mm large magnetite crystals and crystal aggregates  
397 indicates that the ore was deposited as ash. The magmatic origin of the spherule-bearing ore is  
398 supported by its close association with magnetite ore characterized by cavities that resemble  
399 vesicles in lava. Other, unexploited orebodies at El Laco look like lava flows, dikes and  
400 subvolcanic bodies, and their magmatic nature would not be questioned were it not for their  
401 composition. The implication is that less well-preserved deposits of similar ore in other parts of  
402 the world also were derived from iron-oxide melts. Thus, the magnetite spherules at El Laco can  
403 elucidate the controversial origin of the magnetite-apatite ores of Kiruna type.

404  
405

## 406 **ACKNOWLEDGEMENTS**

407  
408 We are grateful to Rosa Anna Fregola, Jennie Gilbert, Ulf Hålenius, Beatriz Levi and Ryan  
409 Mathur for constructive criticism that improved the manuscript. Compañía Minera del Pacífico  
410 (CMP) is thanked for providing facilities at El Laco during several field trips. The study was  
411 supported by Fondo Nacional de Desarrollo Científico y Tecnológico (FONDECYT) grant  
412 1070428, and NSF grant EAR-9814761.

413

414  
415  
416  
417  
418  
419  
420  
421  
422  
423  
424  
425  
426  
427  
428  
429  
430  
431  
432  
433  
434  
435  
436  
437  
438  
439  
440  
441  
442  
443  
444  
445  
446  
447  
448  
449  
450  
451  
452  
453  
454  
455  
456  
457  
458  
459

## REFERENCES CITED

- Ammann, C., Jenny, B., Kammer, K., and Messerli, B. (2001) Late Quaternary Glacier response to humidity changes in the arid Andes of Chile (18-29°S). *Palaeogeography, Palaeoclimatology, Palaeoecology*, 172, 313-326.
- Broman, C., Nyström, J.O., Henríquez, F., and Elfman, M. (1999) Fluid inclusions in magnetite-apatite ore from a cooling magmatic system at El Laco, Chile. *GFF*, 121, 253-267.
- Chou, I.-M., and Eugster, H.P. (1977) Solubility of magnetite in supercritical chloride solutions. *American Journal of Science*, 277, 1296-1314.
- Corona-Esquivel, R., Martínez-Hernández, E., Henríquez, F., Nyström, J.O., and Tritlla, J. (2010) Palynologic evidence for iron-oxide ash fall at La Perla, an Oligocene Kiruna-type iron ore deposit in northern Mexico. *GFF*, 132, 173-181.
- Fregola, R.A., Melone, N., and Scandale, E. (2005) X-ray diffraction topographic study of twinning and growth of natural spinels. *European Journal of Mineralogy*, 17, 761-768.
- Genge, M.J., Engrand, C., Gounelle, M., and Taylor, S. (2008) The classification of micrometeorites. *Meteoritics & Planetary Science*, 43, 497-515.
- Gibbon, D.L., and Tuttle, O.F. (1967) A note on the system FeO-Fe<sub>2</sub>O<sub>3</sub>-SiO<sub>2</sub>-H<sub>2</sub>O. *American Mineralogist*, 52, 886-889.
- Helz G.R. (1971) Hydrothermal solubility of magnetite. PhD Thesis. Pennsylvania State University, Pennsylvania, 220 pp.
- Henríquez, F., and Martin, R.F. (1978) Crystal-growth textures in magnetite flows and feeder dykes, El Laco, Chile. *Canadian Mineralogist*, 16, 581-589.
- Henríquez, F., and Nyström, J.O. (1998) Magnetite bombs at El Laco volcano, Chile. *GFF*, 120, 269-271.
- Henríquez, F., Naslund, H.R., Nyström, J.O., Vivallo, W., Aguirre, R., Dobbs, F.M., and Lledó, H. (2003) New field evidence bearing on the origin of the El Laco magnetite deposit, northern Chile - a discussion. *Economic Geology*, 98, 1497-1500.
- Iyer, S.D., Gupta, S.M., Charan, S.N., and Mills, O.P. (1999) Volcanogenic-hydrothermal iron-rich materials from the southern part of the Central Indian Ocean Basin. *Marine Geology*, 158, 15-25.
- Lefèvre, R., Gaudichet, A., and Billon-Galland, M.A. (1986) Silicate microspherules intercepted in the plume of Etna volcano. *Nature*, 322, 817-820.

- 460 Lindsley, D.H. (1983) Pyroxene thermometry. *American Mineralogist*, 68, 477-493.  
461
- 462 Marini, F., Raukas, A., and Tiirmaa, R. (2004) Magnetic fines from the Kaali impact-site  
463 (Holocene, Estonia): preliminary SEM investigation. *Geochemical Journal*, 38, 107-120.  
464
- 465 McBirney, A.R., and Williams, H. (1979) *Volcanology*. 397 pp. Freeman, Cooper & Co., San  
466 Francisco, CA.  
467
- 468 Meeker, G.P., and Hinkley, T.K. (1993) The structure and composition of microspheres from the  
469 Kilauea volcano, Hawaii. *American Mineralogist*, 78, 873-876.  
470
- 471 Naranjo, J.A., Henríquez, F., and Nyström, J.O. (2010) Subvolcanic contact metasomatism at El  
472 Laco Volcanic Complex, Central Andes. *Andean Geology*, 37, 110-120.  
473
- 474 Naslund, H.R. (1983) The effect of oxygen fugacity on liquid immiscibility in iron-bearing  
475 silicate melts. *American Journal of Science*, 283, 1034-1059.  
476
- 477 Naslund, H.R., Henríquez, F., Nyström, J.O., Vivallo, W., and Dobbs, F.M. (2002) Magmatic  
478 iron ores and associated mineralisation: examples from the Chilean High Andes and Coastal  
479 Cordillera. In T.M. Porter, Ed., *Hydrothermal iron oxide copper-gold & related deposits: a  
480 global perspective*, Vol. 2, 207-226. PGC Publishing, Adelaide, Australia.  
481
- 482 Nyström, J.O., and Henríquez, F. (1994) Magmatic features of iron ores of the Kiruna type in  
483 Chile and Sweden: ore textures and magnetite geochemistry. *Economic Geology*, 89, 820-839.  
484
- 485 Nyström, J.O., Billström, K., Henríquez, F., Fallick, A.E., and Naslund, H.R. (2008) Oxygen  
486 isotope composition of magnetite in iron ores of the Kiruna type in Chile and Sweden. *GFF*,  
487 130, 177-188.  
488
- 489 Park, C.F. Jr. (1961) A magnetite “flow” in northern Chile. *Economic Geology*, 56, 431-436.  
490
- 491 Perry, D.L. (2011) *Handbook of inorganic compounds*, 2nd ed., 581 pp. CRC Press, Boca Raton,  
492 Florida.  
493
- 494 Philpotts, A.R. (1967) Origin of certain iron-titanium oxide and apatite rocks. *Economic  
495 Geology*, 62, 303-315.  
496
- 497 Rhodes, A.L., and Oreskes, N. (1999) Oxygen isotope composition of magnetite deposits at El  
498 Laco, Chile: evidence of formation from isotopically heavy fluids. *Society of Economic  
499 Geologists Special Publication 7*, 333-351.  
500
- 501 Rhodes, A.L., Oreskes, N., and Sheets, S. (1999) Geology and rare earth element geochemistry  
502 of magnetite deposits at El Laco, Chile. *Society of Economic Geologists Special Publication  
503 7*, 299-332.  
504

- 505 Sillitoe, R.H., and Burrows, D.R. (2002) New field evidence bearing on the origin of the El  
506 Laco magnetite deposit, northern Chile. *Economic Geology*, 97, 1101-1109.  
507
- 508 Sokol, E.V., Kalugin, V.M., Nigmatulina, E.N., Volkova, N.I., Frenkel, A.E., and Maksimova,  
509 N.V. (2002) Ferrospheres from fly ash of Chelyabinsk coals: chemical composition,  
510 morphology and formation conditions. *Fuel*, 81, 867-876.  
511
- 512 Sparks, R.S.J., Bursik, M.I., Carey, S.N., Gilbert, J.S., Glaze, L.S., Sigurdsson, H., and Woods,  
513 A.W. (1997) *Volcanic plumes*. 574 pp. John Wiley & Sons, Chichester, England.  
514
- 515 Stankowski, W.T.J., Katrusiak, A., and Budzianowski, A. (2006) Crystallographic variety of  
516 magnetic spherules from Pleistocene and Holocene sediments in the Northern foreland of  
517 Morasko-Meteorite Reserve. *Planetary and Space Science*, 54, 60-70.  
518
- 519 Sulovsky, P. (2002) Mineralogy and chemistry of conventional and fluidised bed coal ashes.  
520 *Bulletin of the Czech Geological Survey*, 77, 1-11.  
521
- 522 Weidner, J.R. (1982) Iron-oxide magmas in the system Fe-C-O. *Canadian Mineralogist*, 20, 555-  
523 566.  
524
- 525 Whitney, J.A., Hemley, J.J., and Simon, F.O. (1985) The concentration of iron in chloride  
526 solutions equilibrated with synthetic granitic compositions; the sulfur-free system. *Economic*  
527 *Geology*, 80, 444-460.  
528
- 529 Zbik, M., and Gostin, V.A. (1995) Morphology and internal structure of Antarctic cosmic dust  
530 spherules: possible links to meteorite fusion crusts. *Proceedings of the National Institute of*  
531 *Polar Research Symposium on Antarctic Meteorites*, 8, 339-351.  
532

533 Figure captions

534

535 FIGURE 1. The El Laco deposits in northern Chile before mining. This study is based on  
536 samples from Laco Sur. An inset shows the location of the open pit (OP) and two outcrops of  
537 “magnetite lava” (L) reported by Park (1961); roads are indicated by thick black lines.

538

539 FIGURE 2. Part of the northwestern wall of the open pit at Laco Sur (bench height = 6 m).  
540 Subhorizontal to shallow-dipping planar structures resembling bedding planes are indicated with  
541 white arrows. Steep structures are gas escape tubes and postdepositional fractures.

542

543 FIGURE 3. Stratification in friable magnetite ore at Laco Sur. A = poorly consolidated ore  
544 without visible apatite; the ore strata are cut by a few steep silica-cemented fractures. B = bedded  
545 ore with thin strata of apatite (cf. figs. 4A-B in Nyström and Henríquez, 1994). C = bedded ore  
546 cut by a gas escape tube (left side); the bedding is best seen at the right side, above two flattened  
547 lumps of orange diadochite and a white apatite layer; the structure of the ore below the  
548 diadochite is obscured by rain-induced flow of ash-sized magnetite; the ore in the central part has  
549 an iridescent blue to purple color due to a film of iron phosphates (undetermined). D = ore with  
550 cross-bedding (the yellowish brown material in the upper right corner is silica colored by  
551 goethite).

552

553 FIGURE 4. Gas escape tubes. A = length-section through a gas escape tube in a block of friable  
554 ore without bedding; a cross-section through the tube is seen at the bottom of the block (in  
555 shadow). B = large magnetite crystals with curved octahedral faces coating a gas escape tube.

556

557 FIGURE 5. SEM images of magnetite spherules in friable iron ore from Laco Sur. A and B =  
558 spherules with concavities (sample LS-57); note the apatite prism at the left side and the thin  
559 magnetite plate in the upper right part of B. C = spherules looking like short cylinders (sample  
560 LS-15). D = ore relatively rich in spherules (sample LS-57); the spherule in the upper central part  
561 is shown in A. E = spherules and octahedral aggregates of magnetite from unconsolidated ore  
562 (sample LS-36). F = spherules in ore with apatite strata (apatite-free portion of sample LS-41).

563

564 FIGURE 6. Magnetite spherules. A = anatomy of a spherule in poorly consolidated ore (sample  
565 LS-58), showing an aggregate of octahedra with partial, subparallel overgrowth of magnetite. B  
566 = spherule with concavities (sample LS-57). C and D = spherules with concavities and curved  
567 outline generated by stepwise, subparallel overgrowth of magnetite; the tiny drop-like bodies on  
568 the magnetite consist of late silica (sample LS-15). E = magnetite crystals decorated with  
569 projecting magnetite lamellae of bladeliike form along octahedral planes (sample LS-57); the  
570 bladeliike magnetite also occurs as small rosettes. F = magnetite decorated with bands of  
571 magnetite lamellae, and an overgrown roselike cluster of euhedral hematite plates in the central  
572 part (sample LS-58).

573

574 FIGURE 7. A = magnetite decorated with magnetite lamellae (sample LS-57). B = apatite prisms  
575 decorated with bladeliike magnetite lamellae, oriented along the *c*-axis, and forming small  
576 rosettes (sample LS-57). C = spherule composed of tabular magnetite crystals (inset shows  
577 magnified part; sample LS-58). D = euhedral, partly corroded hematite crystals from

578 unconsolidated, stratified ore in a roadcut 100-200 m southwest of the open pit (Fig. 1; sample  
579 LS-25D).

**Fig. 1**

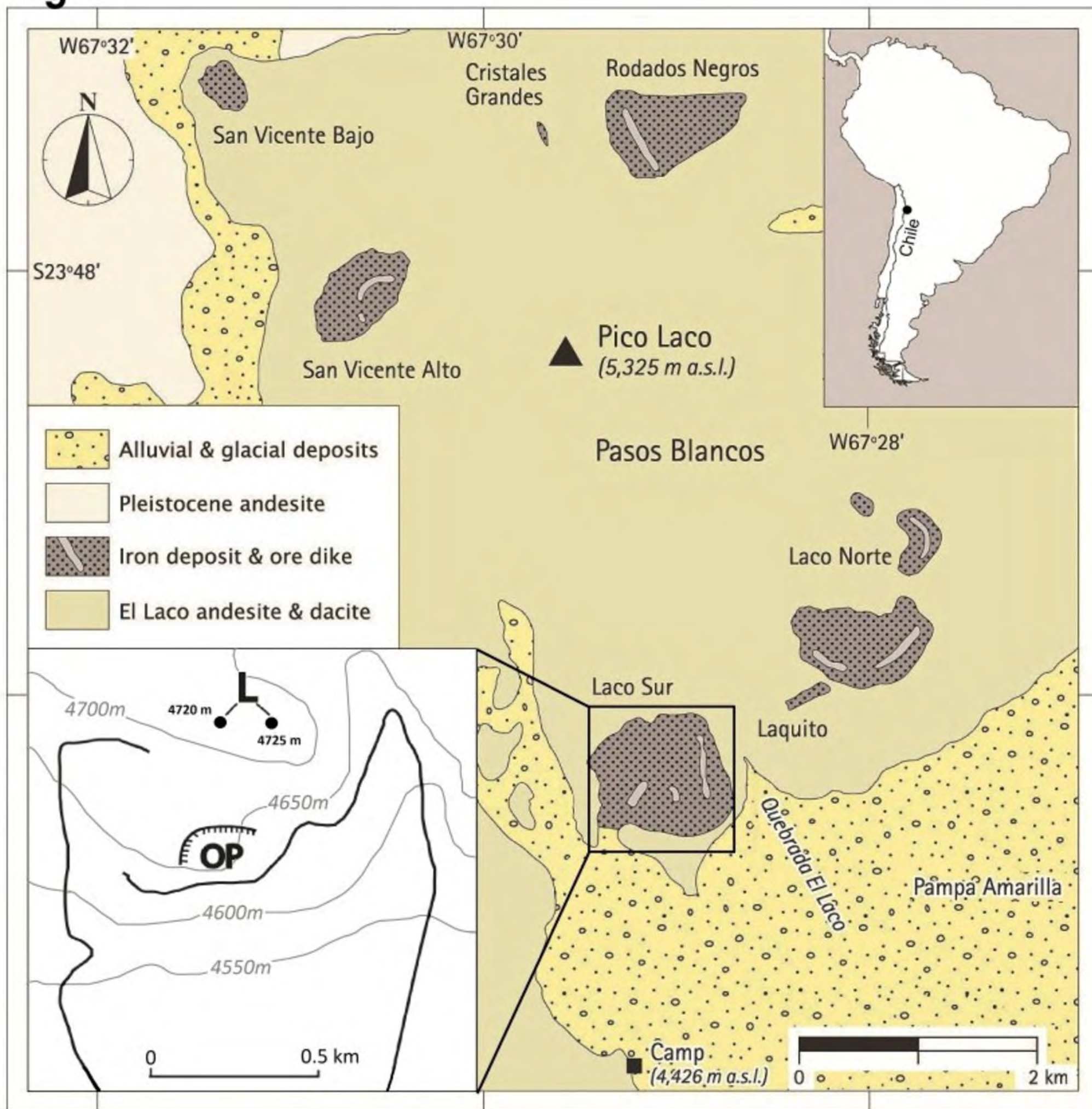


Fig. 2

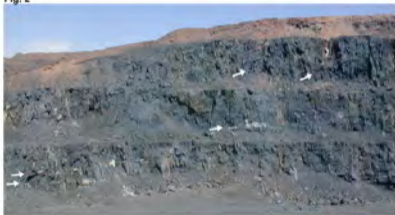




Fig. 3A



Fig. 3B



Fig. 3C



Fig. 10



Fig. 4A



Fig. 4B



Fig. 5

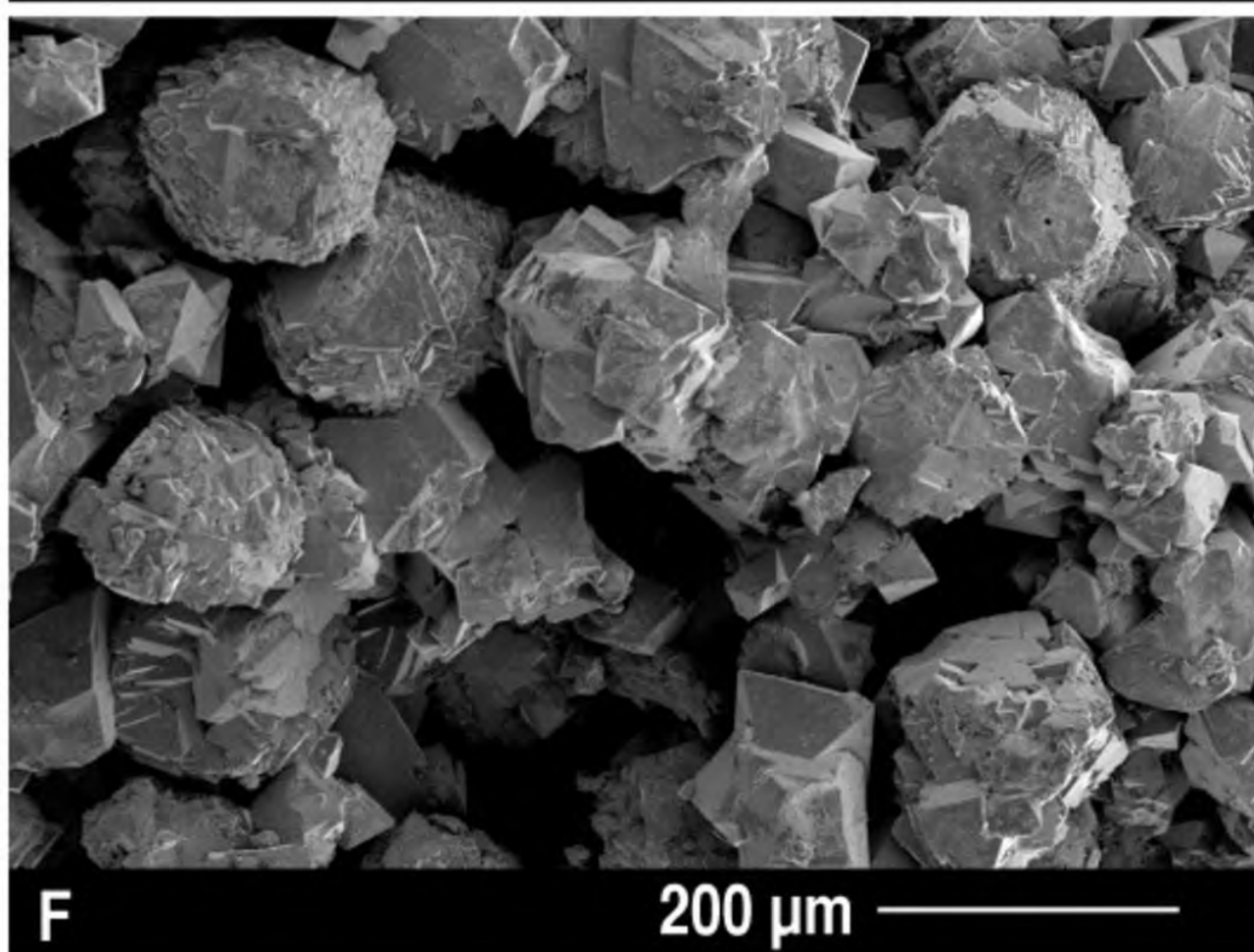
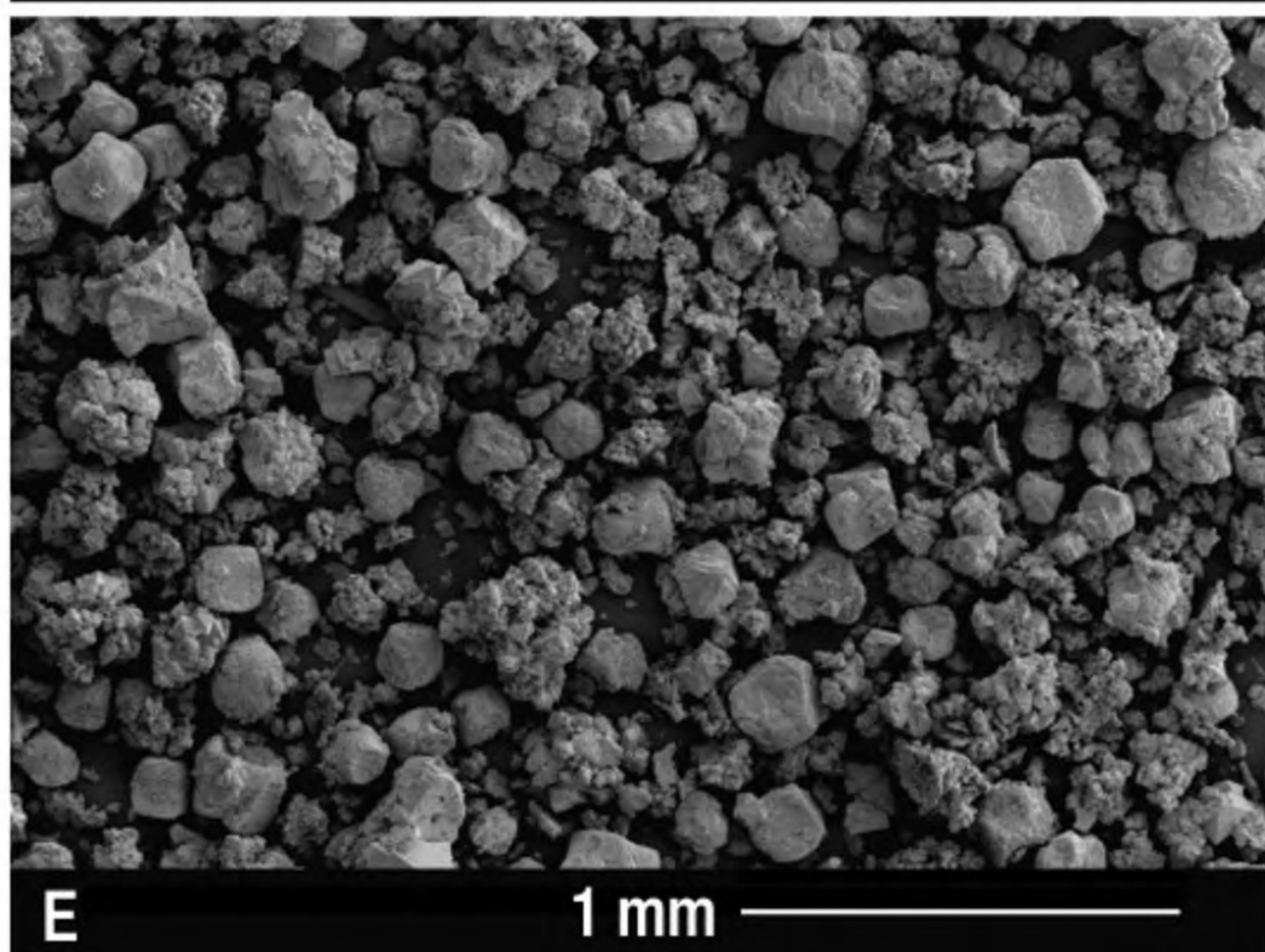
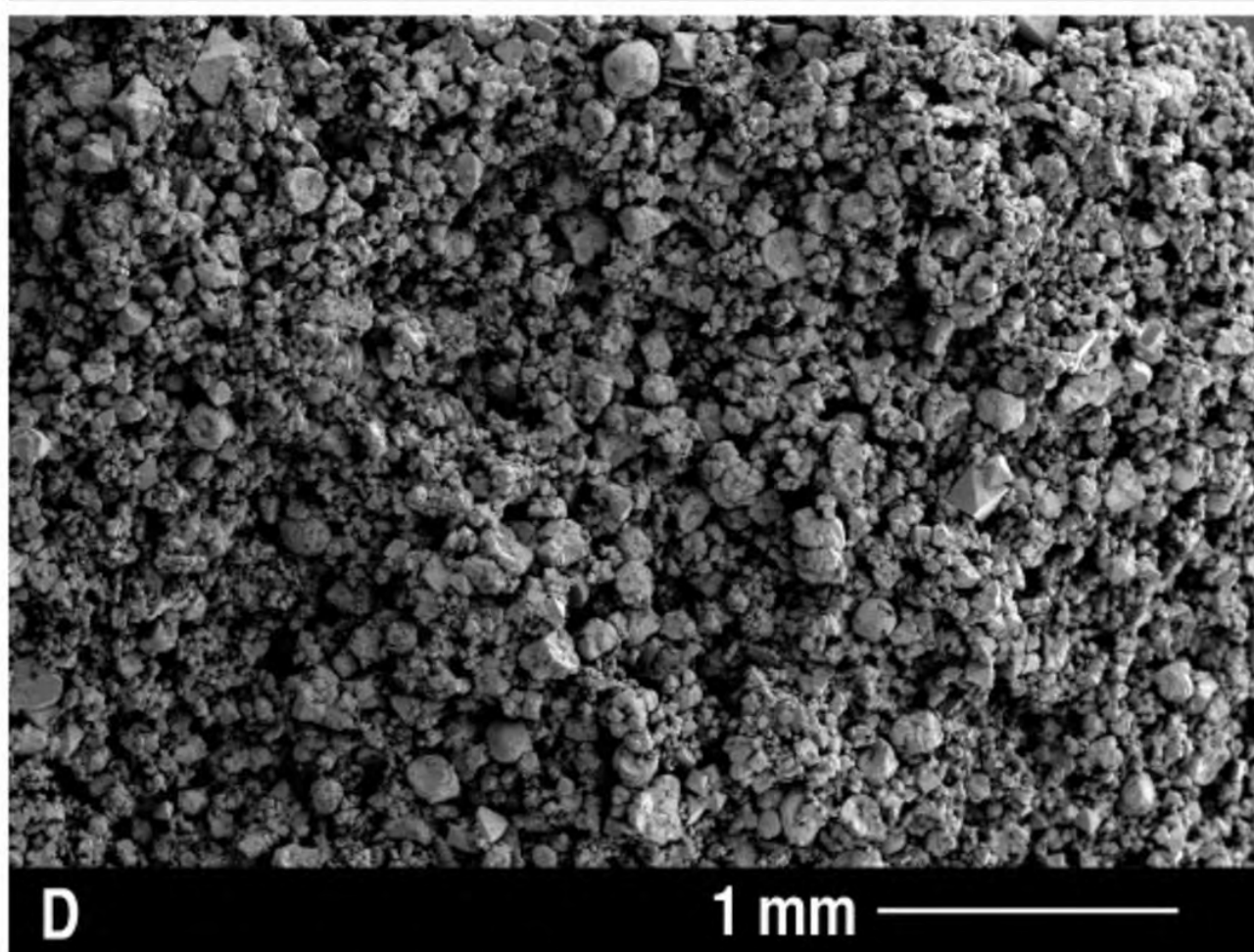
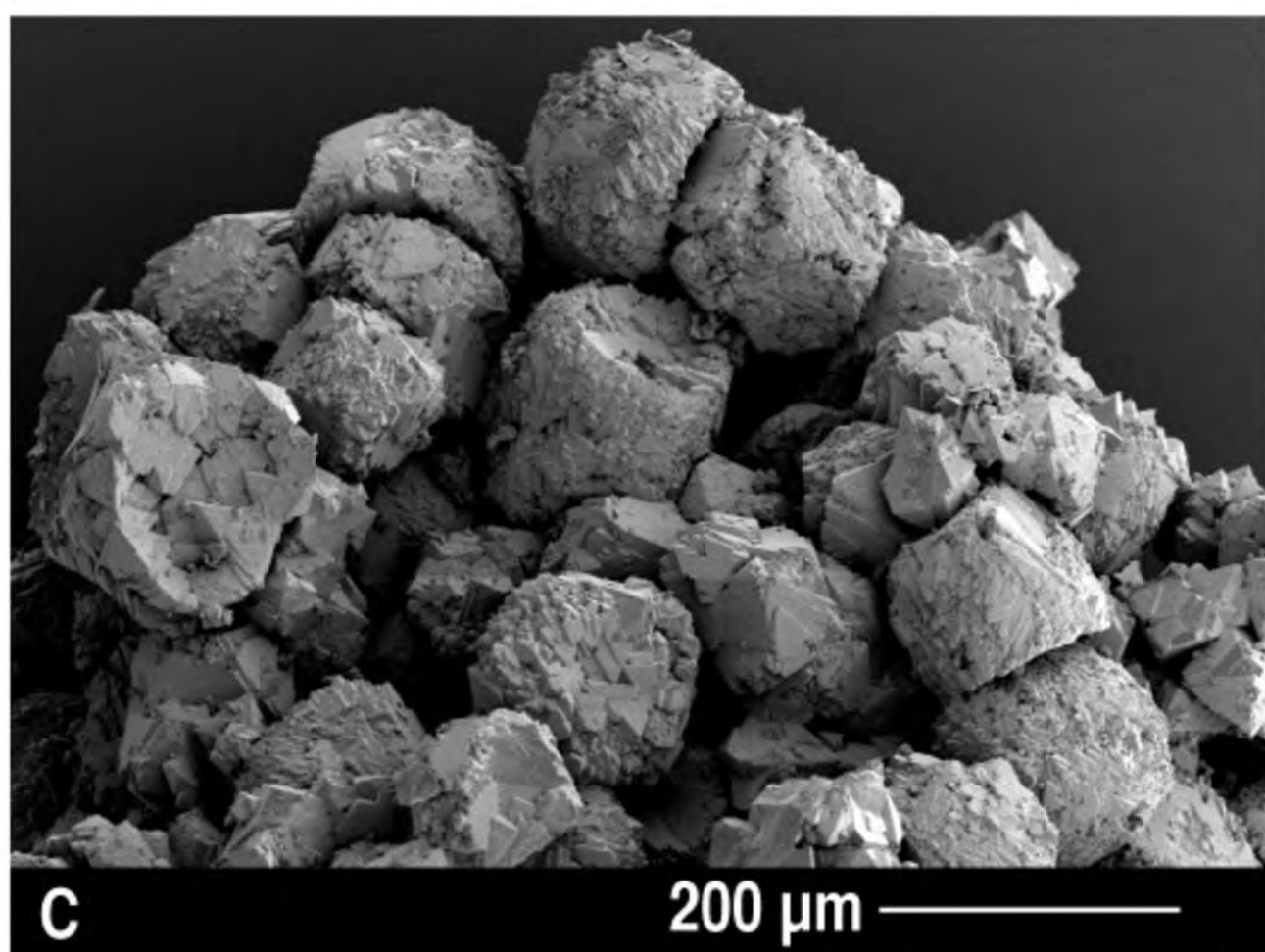
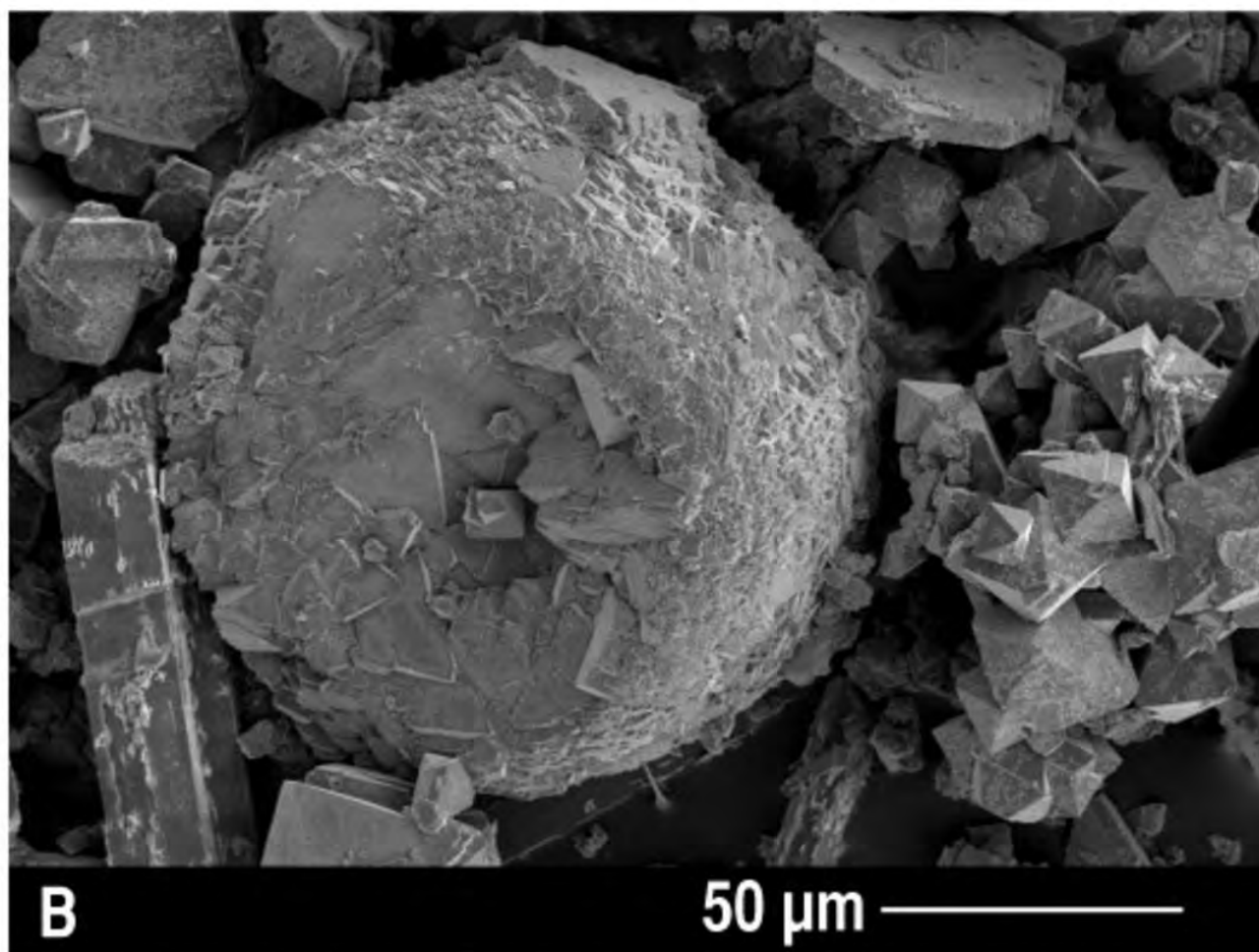
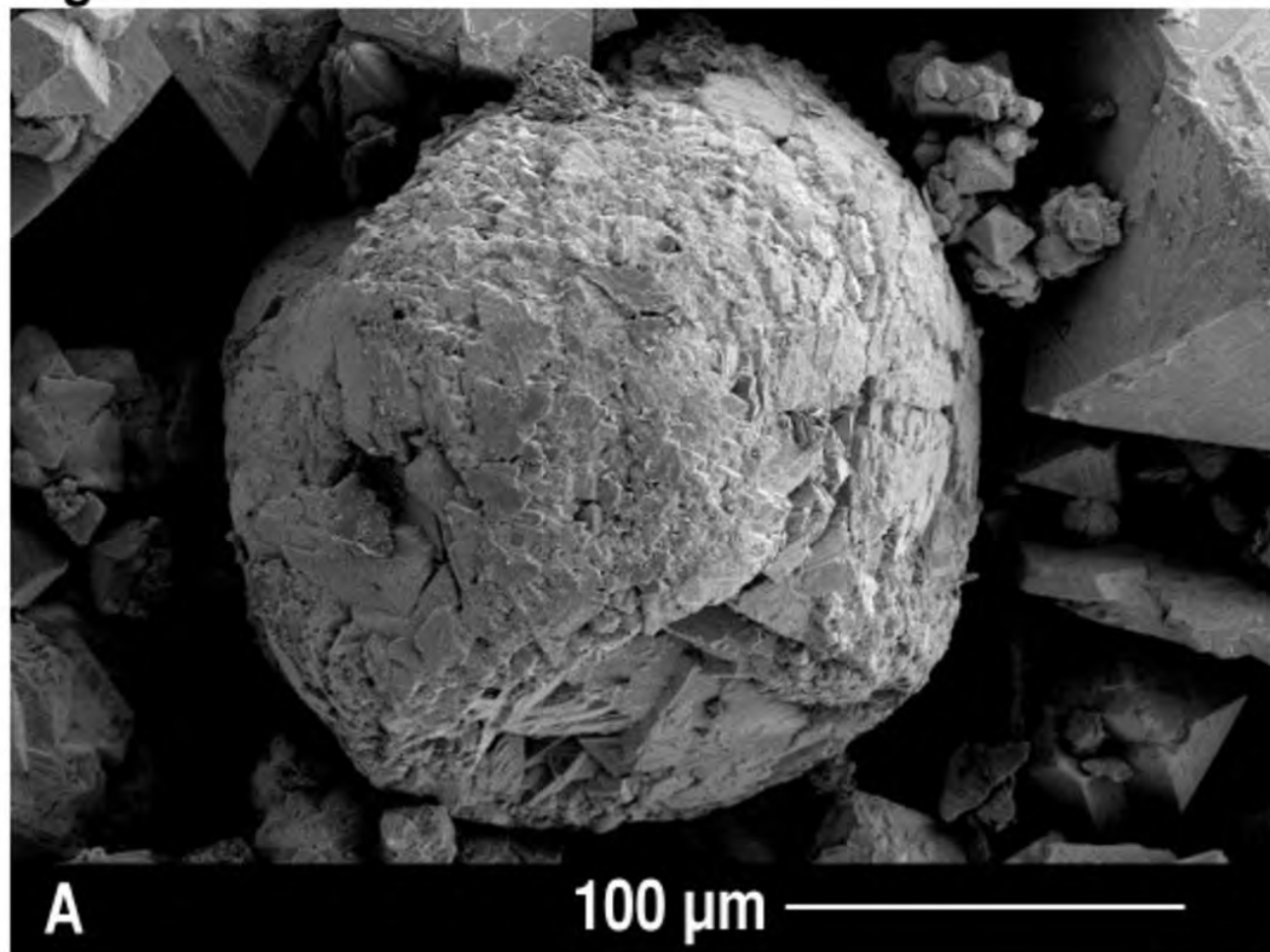


Fig. 6

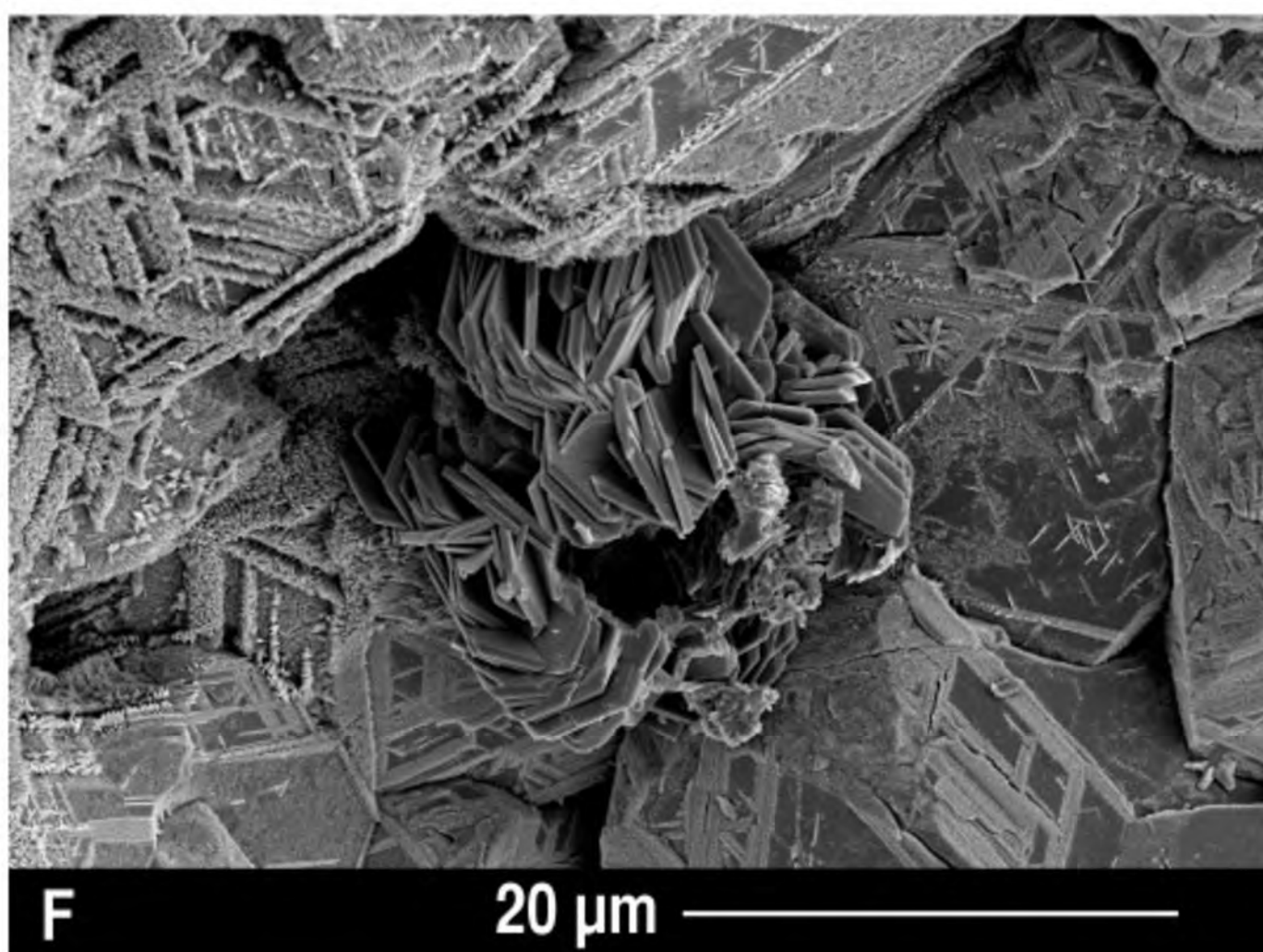
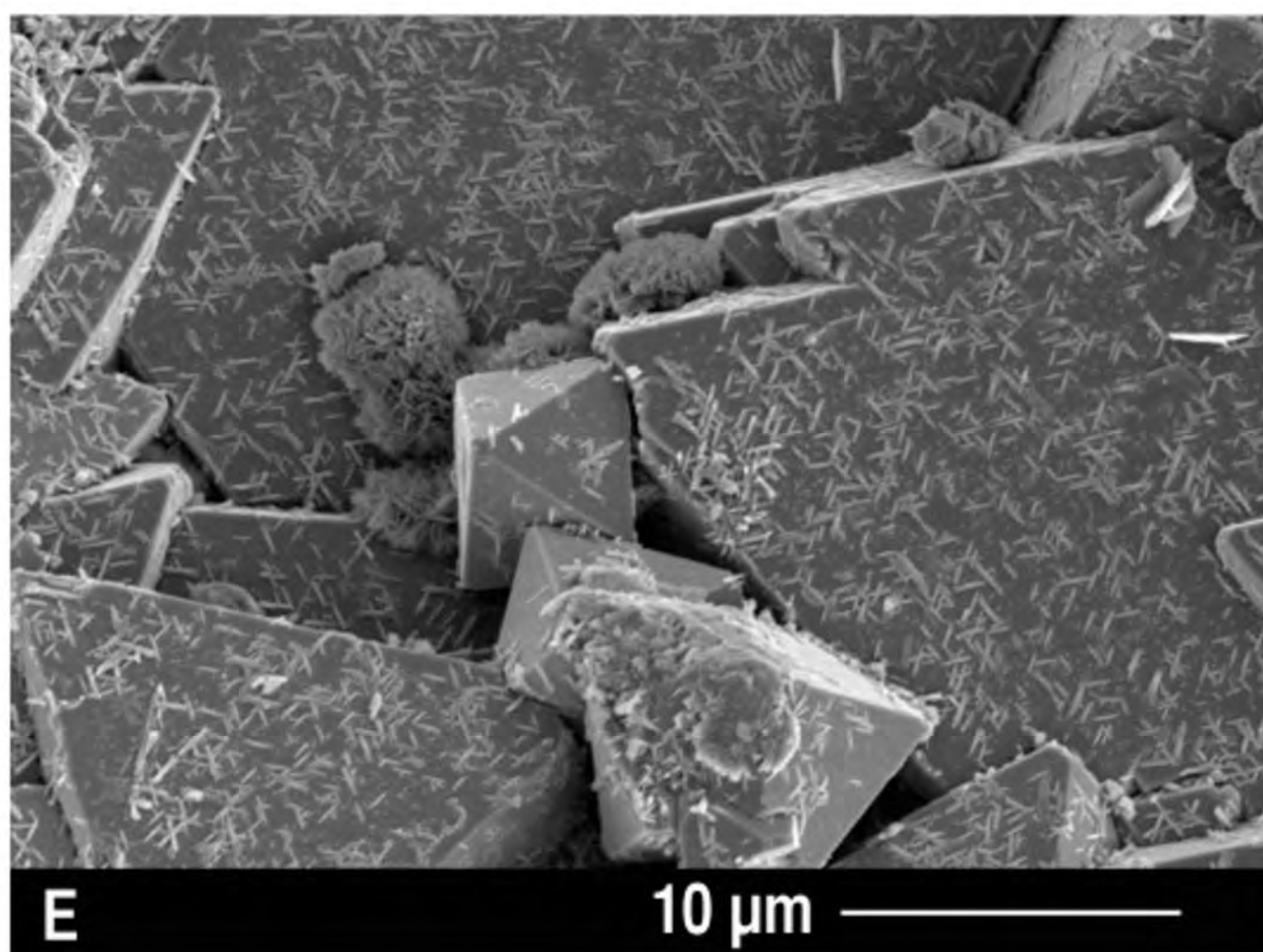
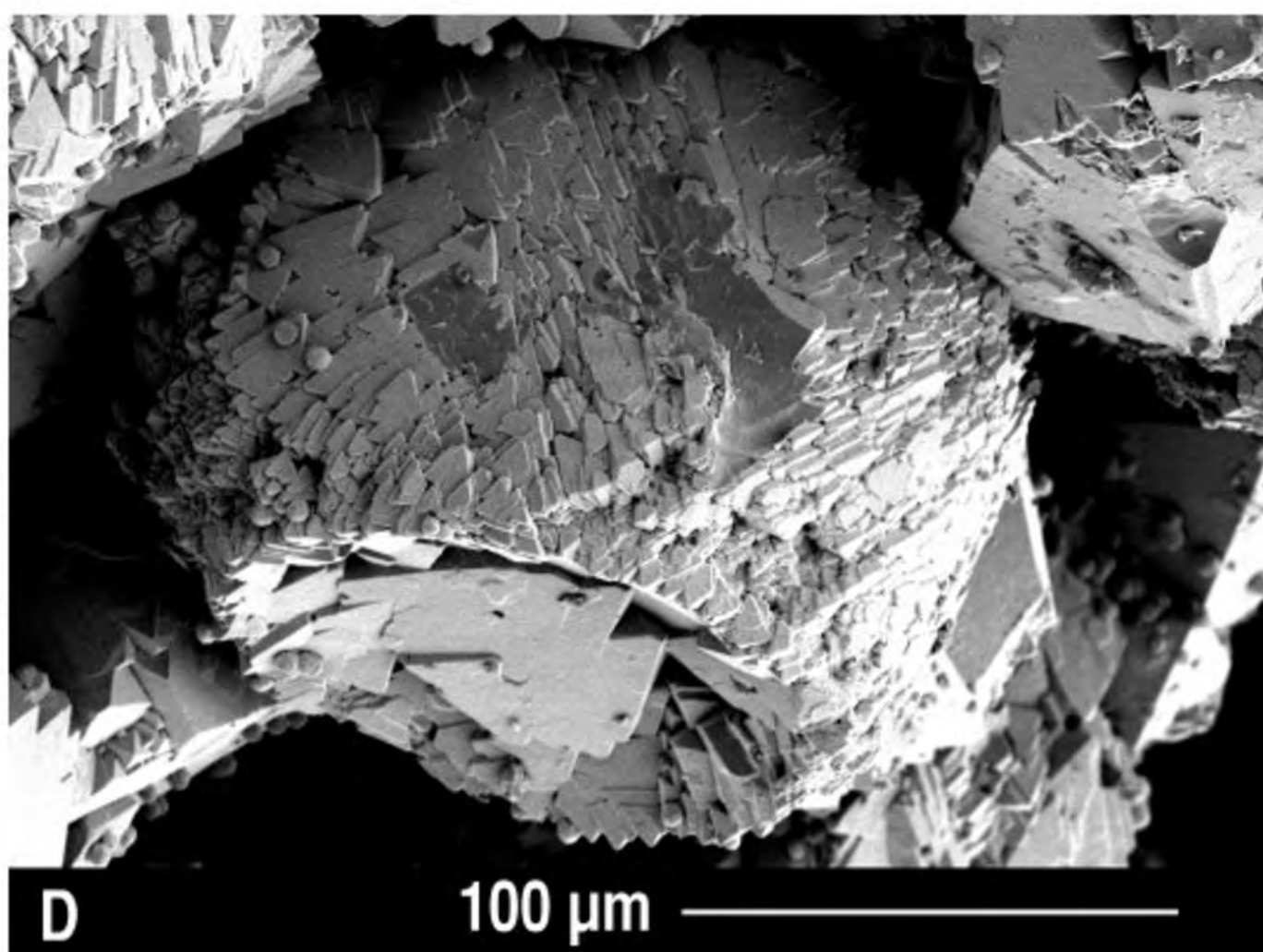
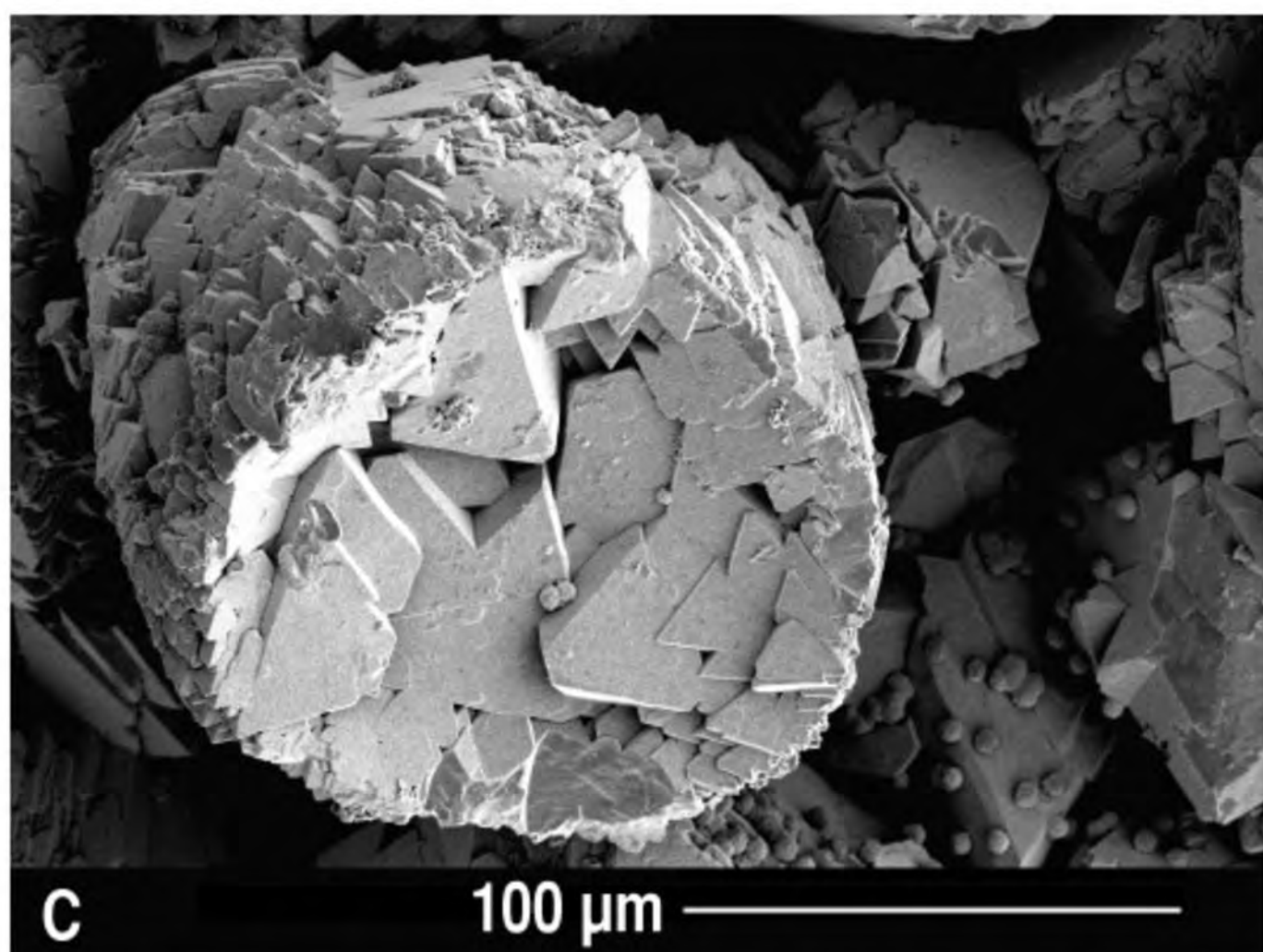
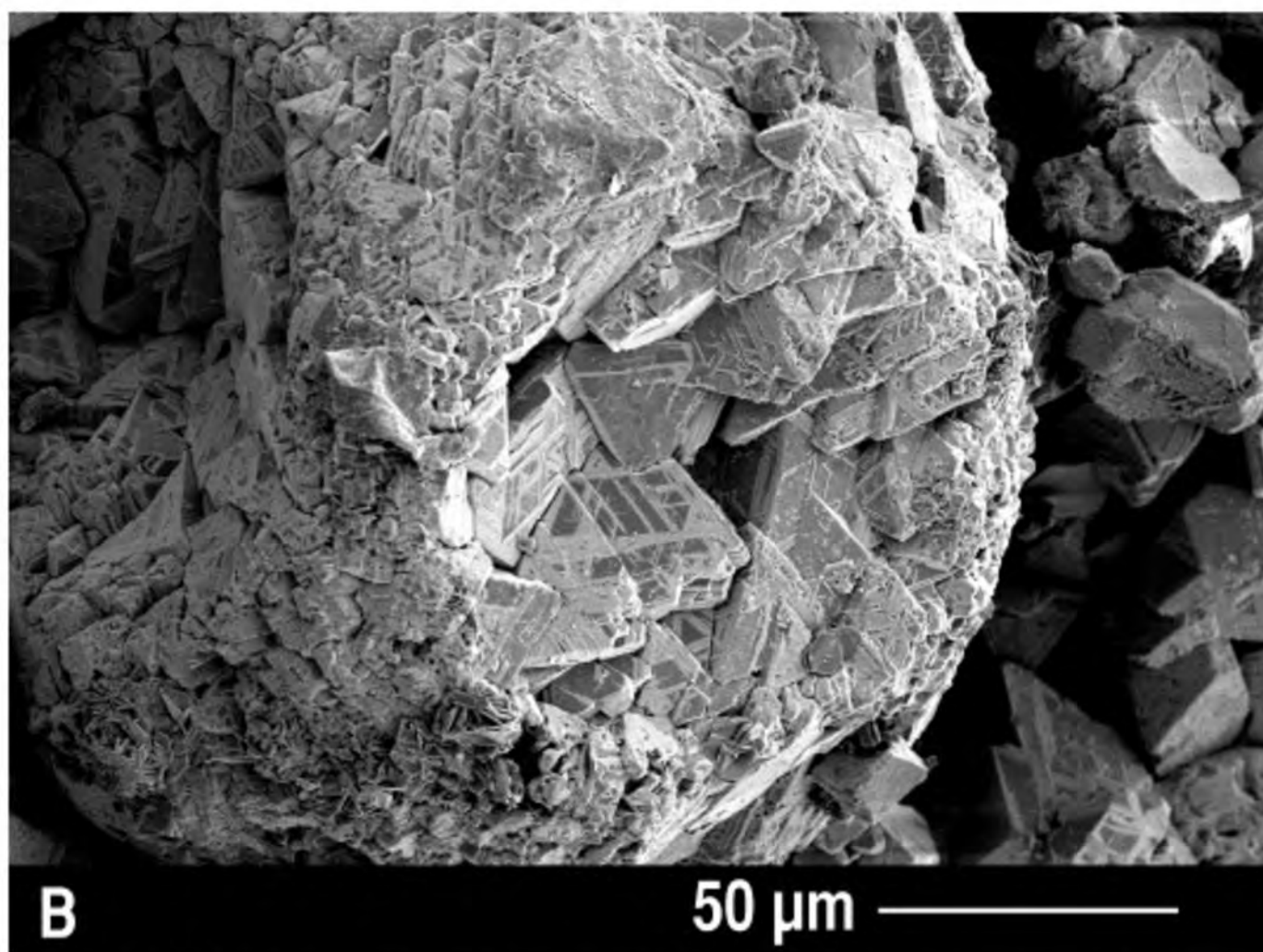
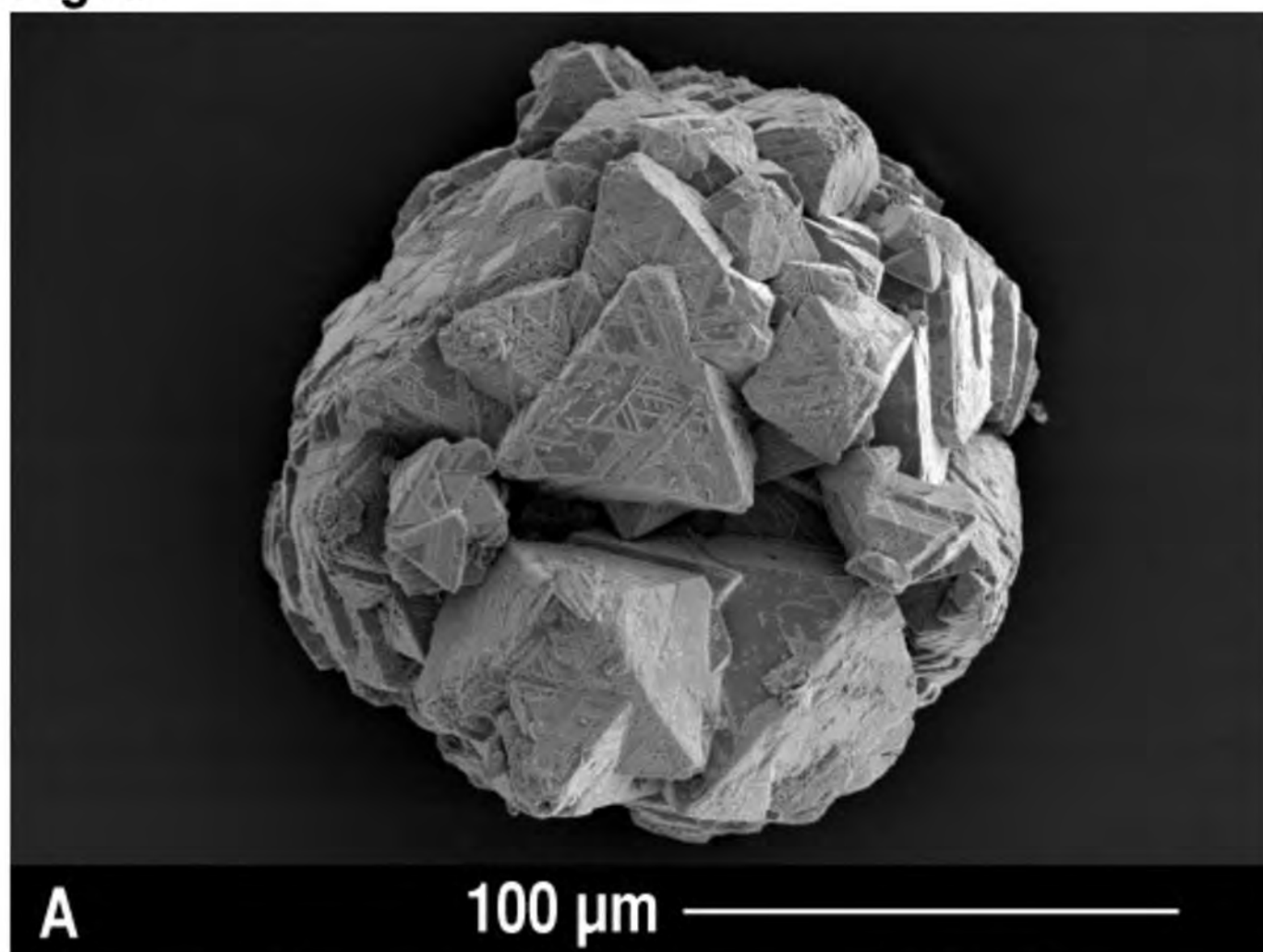




Fig. 7

